

# Sensing of remote oxyanion binding at the DNA binding domain of the molybdate-dependent transcriptional regulator, ModE

David H. Boxer,<sup>\*a</sup> Han Zhang,<sup>a</sup> David G. Gourley,<sup>a</sup> William N. Hunter,<sup>a</sup> Sharon M. Kelly<sup>b</sup> and Nicholas C. Price<sup>b</sup>

<sup>a</sup> Division of Biological Chemistry and Molecular Microbiology, School of Life Sciences, University of Dundee, Dundee, UK DD1 5EH

<sup>b</sup> Division of Biochemistry and Molecular Biology, Faculty of Biomedical and Life Sciences, Glasgow University, Glasgow, Scotland, UK G12 8QQ

Received 19th March 2004, Accepted 26th May 2004

First published as an Advance Article on the web 1st September 2004

The molybdate-dependent transcriptional regulator ModE of *Escherichia coli* displays a large (50%) quenching of its intrinsic tryptophan fluorescence on binding molybdate. The changes in fluorescence have been exploited to analyse the binding of molybdate to ModE. Utilising site-directed mutagenesis, a series of phenylalanine substitutions for the three tryptophans of ModE (Trp49, Trp131 and Trp186) have been constructed, to yield three mono-Trp-containing derivatives. This has allowed an assessment to be made of the contribution of each of the three tryptophans to the spectral changes observed on binding molybdate; these are most distinctive for Trp186. Linkage between the DNA-binding and molybdate-binding sites (some 55 Å apart) is shown by (a) the small, but definite, effect of molybdate on the fluorescence of Trp49 which is located at the DNA-binding winged helix–turn–helix domain, and (b) the finding that the binding of either ligand is enhanced in the presence of the other. The studies demonstrate that the mono-Trp derivatives of ModE could be useful tools with which to study the signal transduction processes specifically associated with molybdate-dependent transcriptional regulation and that this approach may have wider implications for analysis of other regulated systems.

## Introduction

The molybdate-dependent transcriptional regulator protein ModE is the principal means of controlling bacterial molybdenum metabolism.<sup>1–7</sup> When ModE is activated by binding molybdate, it limits molybdenum uptake by repressing the molybdate transporter operon *modABCD*. However, ModE also enhances the transcription of enzymes encoded by the *moaABCDE* operon, which are involved in molybdenum–cofactor biosynthesis pathways as well as of molybdenum-dependent enzymes.

ModE from *Escherichia coli* is a dimer with each polypeptide chain consisting of 262 amino acids. X-ray structures have been determined for apo-ModE,<sup>8</sup> the isolated molybdate-binding domain complexed with molybdate,<sup>9</sup> and recently for intact ModE complexed with molybdate.<sup>10</sup> ModE consists of four structural regions (Fig. 1). The N-terminal domain DNA-binding domain (residues 1–103) is predominantly  $\alpha$ -helical with a winged helix–turn–helix (wHTH) motif contributed by each chain. A flexible linker region (residues 104–119) connects the DNA-binding and the molybdate-sensing parts of the molecule. The molybdate-binding domain consists of two tandem repeats of the so-called mop domains (residues 120–187 and 188–262), Greek key  $\beta$ -barrels similar to the oligonucleotide/oligosaccharide binding fold.<sup>8</sup> There are three Trp residues in ModE (see Fig. 1), one of which (Trp49) is located at the DNA-binding site, and another of which (Trp186) is close to the molybdate-binding site.

The binding of molybdate to ModE induces significant structural changes within the molybdate-binding domain (Fig. 1(c) and (d)).<sup>9,10</sup> In essence, these changes consist of rigid body movements of the two mop domains in each polypeptide chain against each other which, together with the movement of loops within the domains, leads to a significant reduction in exposed surface area on binding molybdate. The changes lead to the loss of the pronounced asymmetry of the apo-ModE structure.<sup>8</sup> As indicated in Fig. 1(c) and (d) there is a significant change in the mutual orientation of the Trp186 side chains of each polypeptide on binding molybdate. Although some of the structural changes which occur on binding molybdate are understood, there is less information about the extent to which these are transmitted to the DNA-binding site. This reflects, in part the significantly lower resolution of diffraction data that could be

obtained for the ModE–molybdate complex as well as the failure to obtain ordered crystals of the ternary ModE–molybdate–DNA complex.<sup>10</sup>

Binding of molybdate to ModE leads to a significant (50%) quenching of the intrinsic Trp fluorescence of the protein.<sup>3</sup> It also brings about distinct changes in the near UV CD spectrum around 290 nm, the region characteristic of tryptophan side chains, with little change in the far UV CD indicating little change in secondary structure content. The changes in fluorescence have been used to determine the stoichiometry and  $K_d$  for the ModE–molybdate interaction. We now describe the construction and characterisation of a series of ModE derivatives in each of which only one of the tryptophan residues is retained. This has allowed us to dissect the contribution made by each Trp to the observed spectral changes in ModE and to assess the extent of the communication between the oxyanion and DNA binding sites. The results indicate that ModE should serve as a useful model system for studying the molecular mechanisms involved in intramolecular signalling and transcriptional regulation.

## Results

### Properties of the mono-(Phe-Trp)-substituted ModE derivatives

ModE possesses three tryptophans, Trp49, Trp131 and Trp186. Trp49 is located at the HTH motif of the DNA-binding, N-terminal domain of the molecule, and close to the DNA-binding site. Trp131 is at the core of the first of the mop domains in the C-terminal molybdate-binding protein of the molecule. Trp186 is situated towards the C-terminal end of the first mop domain and is exposed at the surface of this sub-domain. In the crystal structure of the dimeric ModE, Trp186 is at the mop–mop interface.<sup>8</sup> Unusually, the two Trp186 residues are asymmetrically arranged in the apo-ModE structure (Fig. 1(c)).

Initial site-directed mutagenesis experiments aimed to assess the consequences for ModE function as a transcriptional activator, of replacing independently each of the tryptophan residues with phenylalanine. The genetic complementation test (see Experimental) was devised to assess the ability of plasmid-borne clones of mutated

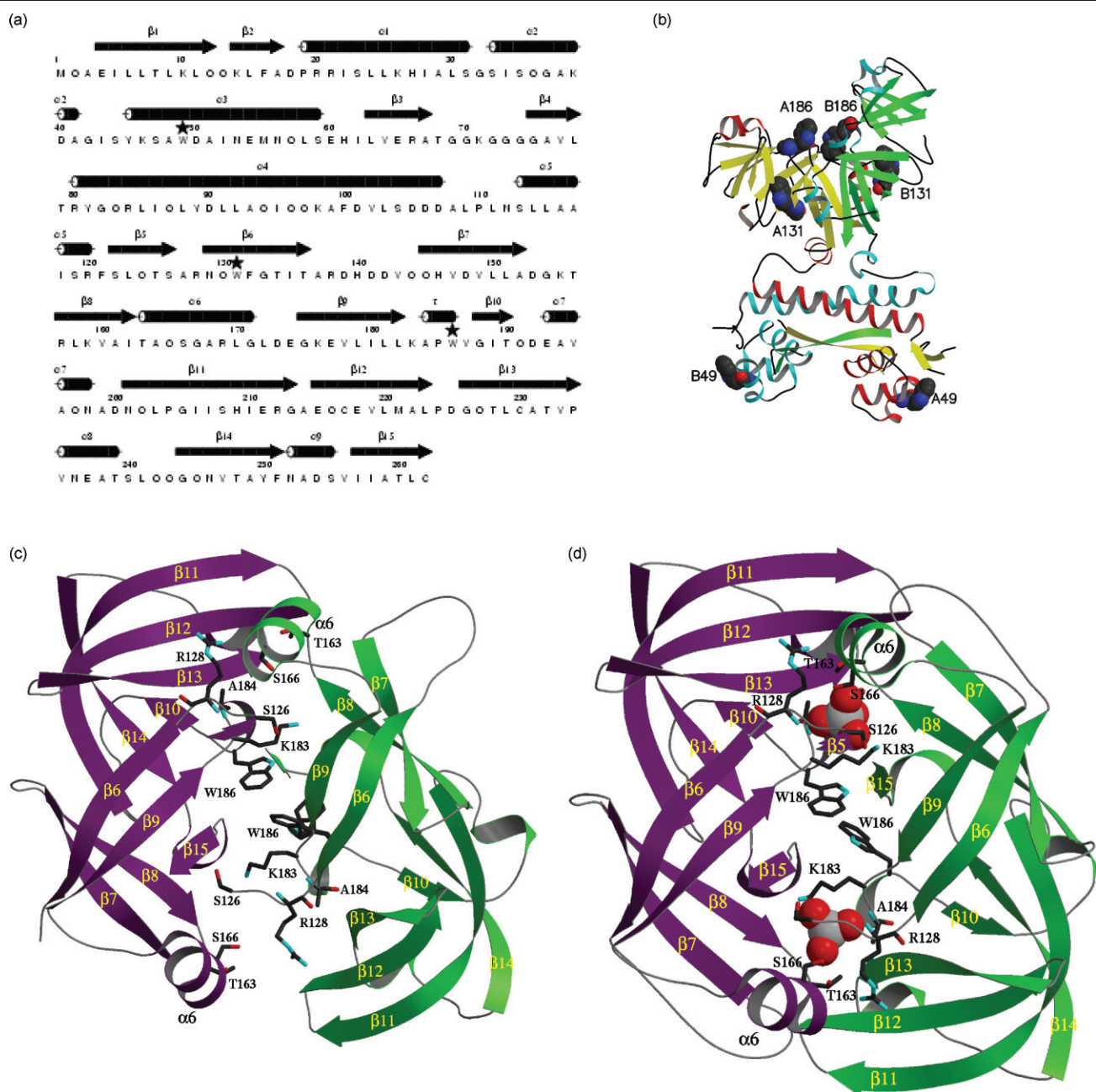


**Fig. 1** Sequence and structure of ModE. (a) The amino acid sequence of *E. coli* ModE with the assigned secondary structure.  $\tau$  identifies a short segment of  $3_{10}$ -helix and asterisks mark the positions of the three tryptophans (Trp49, Trp131 and Trp186). (b) The structure of the ModE dimer. The  $\alpha$ -helices and  $\beta$ -strands of subunit A are coloured red and yellow, respectively, in subunit B cyan and green, respectively. The tryptophan residues are depicted as CPK models (C coloured black, N blue and O red) and labelled. The DNA-binding domain is at the bottom of the image, the oxyanion-binding domain at the top. (c) A view into the oxyanion-binding site of the dimop domains prior to loading with molybdate. Subunit A is coloured purple, B green. Side chains of selected residues are shown as sticks coloured C black, N cyan, O red. (d) The same view as in (c) for the molybdate complex. Molybdate is shown as a CPK model coloured Mo grey, O red. This figure was prepared using the programs ALINE<sup>23</sup> and MOLSCRIPT.<sup>24</sup>

*ModE* to express functional ModE. ModE is a positive transcriptional regulator of the *moa* operon.<sup>3</sup> The ability of pET15b clones carrying mutated *ModE*, to restore the expression of  $\beta$ -galactosidase from a (*moa::lacZ*) fusion in a *modE* strain (strain LA29) indicates that the mutated ModE retains its function. Mutation of Trp131 and Trp186 independently to phenylalanine was without effect on the function of ModE. Mutation of Trp49 to phenylalanine, however, led to the loss of the ability of ModE to activate *moa* transcription. This is consistent with Trp49 being located in the proximity of the DNA-binding site. The presence of the N-terminal His-tag extension as a consequence of its expression from the pET15b vector, had no effect on either the genetic complementation test or the *in vitro* measurements of molybdate and DNA binding to the isolated His-tagged ModE.<sup>3</sup> Each of the mono-substituted (Trp $\rightarrow$ Phe) ModE derivatives was purified and all, including the inactive W49F ModE, retained the ability to bind molybdate in a similar manner to the unmodified ModE (data not shown).

### Construction and characterisation of the mono-Trp derivatives of ModE

Starting from the mono-Trp $\rightarrow$ Phe substituted ModE derivatives, further site-directed mutagenesis was undertaken to construct the three di-(Trp $\rightarrow$ Phe) ModE derivatives, each of which possess a single tryptophan at one of the three positions, namely Trp49, Trp131 and Trp186. For convenience, and in order to emphasise the identity of the Trp present in each of these di-substituted derivatives, the double mutants (i) W131F, W186F, (ii) W49F, W186F and (iii) W49F, W131F are referred to in this paper as (i) W49-ModE, (ii) W131-ModE, and (iii) W186-ModE, respectively.

Assessment of the ability of these mutated ModE molecules to function in the activation of *moa* expression, revealed that only the W49-ModE was functional. This is consistent with the previous finding that substitution of Phe for Trp at position 49 leads to inactivation.

The UV-absorption spectra of these three derivatives were similar in the 270 to 300 nm region. Compared with wild-type ModE, each derivative showed the expected reduced level of absorption due to the replacement of Trp, but the spectra showed additional fine structure. The absorption maximum for both the W131- and W186 derivatives was 277 nm and two similar pronounced shoulders at 288 and 293 nm were also apparent. The W49-ModE displayed an absorption maximum at 276 nm; however there was a smaller shoulder at 288 nm, than found for the other mono-Trp derivatives and no irregularity at 293 nm was evident, pointing to subtle differences in the electronic environment of Trp49 compared with the other two Trp side chains in the protein (data not shown).

The far UV CD spectrum of each of the mono-Trp derivatives (Fig. 2) was very similar to that of unmodified ModE previously reported.<sup>3</sup> This is consistent with each of the mono-Trp derivatives having an overall secondary structure similar to that of the unmodified ModE.

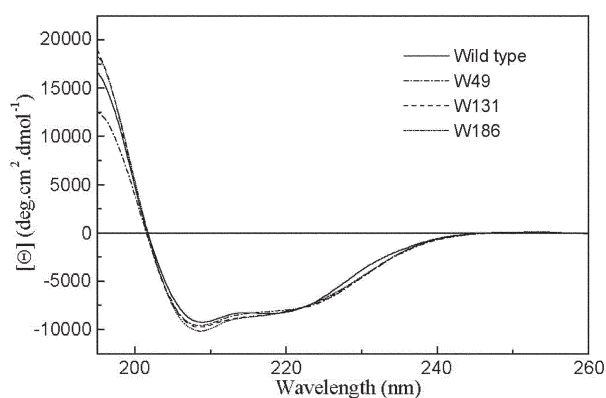


**Fig. 2** Far UV CD spectra of ModE and derivatives. Spectra were recorded at a protein concentration of 17.6  $\mu\text{M}$  (0.5  $\text{mg ml}^{-1}$ ) in 50 mM Tris/HCl, pH 7.6, at 20 °C in a cell of pathlength 0.02 cm. Spectra were truncated below 195 nm because of excessive noise at these wavelengths.

### Fluorescence properties of the mono-Trp-ModE derivatives

The origin of the unusually large degree of quenching (50%) of the overall ModE tryptophan fluorescence on binding molybdate,<sup>3</sup> is now amenable to dissection by analysis of the three mono-Trp derivatives. The composite Fig. 3 displays the fluorescence spectra of each of the mono-Trp derivatives along with the unmodified ModE (Fig. 3(a)) for comparison. The spectrum for each derivative is recorded both in the absence and presence of molybdate (0.5 mM).

The emission spectrum of the non-functional, W186-ModE derivative exhibits a lower fluorescence yield than the average for the three tryptophans in ModE and an unusually low maximum wavelength of 325 nm (Fig. 3(b)). The low emission maximum would be consistent with a low degree of exposure to solvent<sup>11</sup> but in view of the crystal structure of apo-ModE,<sup>8</sup> the magnitude of the shift to lower wavelengths is strongly indicative of additional factors being involved. The unusual asymmetry of the two Trp186 residues in the ModE dimer, their close proximity and relative geometry could contribute to the distinct fluorescence emission spectral features. On addition of molybdate a very large degree of quenching (about 70%) was observed, to yield a broad, rather featureless, spectrum with an emission maximum of about 340 nm. Therefore, despite being inactive in the transcriptional regulation of *moa*, the molecule retains the ability to interact with molybdate. This is as expected since the mutation of Trp49 to Phe, which inactivates ModE as a transcriptional regulator, almost certainly affects the interaction of the protein with DNA.

Fig. 3(c) shows the fluorescence emission spectrum of W131-ModE. The maximum wavelength for the spectrum for the apo-protein is 354 nm and the fluorescence intensity is larger than the average of the three tryptophans in the protein. The emission maximum is typical of a tryptophan residue in a globular protein with a high degree of exposure to solvent.<sup>11</sup> A marked degree of quenching of the emission spectrum (about 30%) was observed in the presence

of molybdate, accompanied by a blue shift of the emission maximum to 345 nm. Like W186-ModE, W131-ModE is biologically non-functional, due to the mutation of Trp49 yet retains its ability to bind molybdate. While the environment of Trp131 in ModE clearly changes in the presence of molybdate, its fluorescence emission spectrum is quite distinct from that of W186-ModE.

The fluorescence emission spectrum of W49-ModE in the absence of molybdate displays a maximum at 348 nm and a fluorescence yield below the average for the three tryptophans in ModE. The emission maximum suggests a slightly decreased exposure to solvent in comparison with W131-ModE; this observation is consistent with the crystal structure of ModE.<sup>8</sup> The addition of molybdate produced a small (5%), but definite, enhancement of the fluorescence emission without significant change in the emission maximum (Fig. 3(d)). W49-ModE is the only mono-Trp-ModE derivative which retains its biological activity in effecting molybdate-dependent enhancement of *moa* transcription. It must, therefore, retain its ability to bind molybdate. This is explored further below.

The internal consistency of these results could be assessed by comparing the additive combined spectra of the three mono-Trp derivatives (Fig. 3(e)) with the emission spectra found for wild-type ModE both in the absence and presence of molybdate (Fig. 3(a)). In the absence of molybdate the intensity of the combined spectrum is approximately 15% lower than that of unmodified ModE, whereas in the presence of molybdate the intensity of the combined spectrum is some 20% higher than that of the unmodified ModE. These discrepancies (when taken together with the small (2 nm) differences in the emission maxima) likely reflect interactions which may occur between Trp186 and Trp131. There may also be subtle local structural differences between the mutants and wild-type ModE which affect the environments of the individual tryptophan residues.

The fluorescence data just described clearly indicate that Trp186 in apo-ModE is in an unusual environment that is substantially changed on binding molybdate, making the most marked contribution to the overall molybdate-induced quenching of ModE fluorescence. Furthermore, the small but definite changes in the fluorescence of Trp49 observed on addition of molybdate suggest that the conformational change in the wHTH region of the DNA binding domain (Fig. 1), is brought about by interaction with molybdate at a remote site on the other domain of the molecule.

### Near UV CD spectra of the mono-Trp-ModE derivatives

The addition of molybdate to ModE leads to marked changes in the CD spectrum in the region between 285 and 300 nm,<sup>3</sup> a region where bands arise predominantly from tryptophan side chains.<sup>12,13</sup> On addition of molybdate the rather broad spectrum of apo-ModE becomes much sharper, although the value of the ellipticity at the minimum (292 nm) is not significantly changed (Fig. 4(a)). We explored the contributions of the three tryptophan side chains to the molybdate-induced spectral change by examining the behaviour of the single Trp-containing mutants.

The near UV CD spectra of W186-ModE, W131-ModE and W49-ModE derivatives in the presence and absence of molybdate are shown in Fig. 4(b), (c) and (d), respectively. In the cases of the W186-ModE and W131-ModE derivatives, the spectra in the 285 to 300 nm region are relatively broad in the absence of molybdate, and become sharper on addition of ligand. In the case of the W186-ModE derivative, the addition of molybdate does not lead to a significant change in ellipticity at 292 nm (Fig. 4(b)), but there is a marked decrease in ellipticity at this wavelength on addition of molybdate to the W131-ModE derivative (Fig. 4(c)).

By contrast, the W49-ModE derivative shows only a very small CD signal in the region characteristic of tryptophan and there is no significant change on addition of molybdate. The small CD signal suggests that the Trp49 side chain is not highly constrained within the asymmetric tertiary fold of the protein. This would be consistent with the relatively high degree of exposure of Trp49 to the solvent indicated by the fluorescence emission maximum (348 nm) of the W49-ModE derivative (Fig. 3(d)).

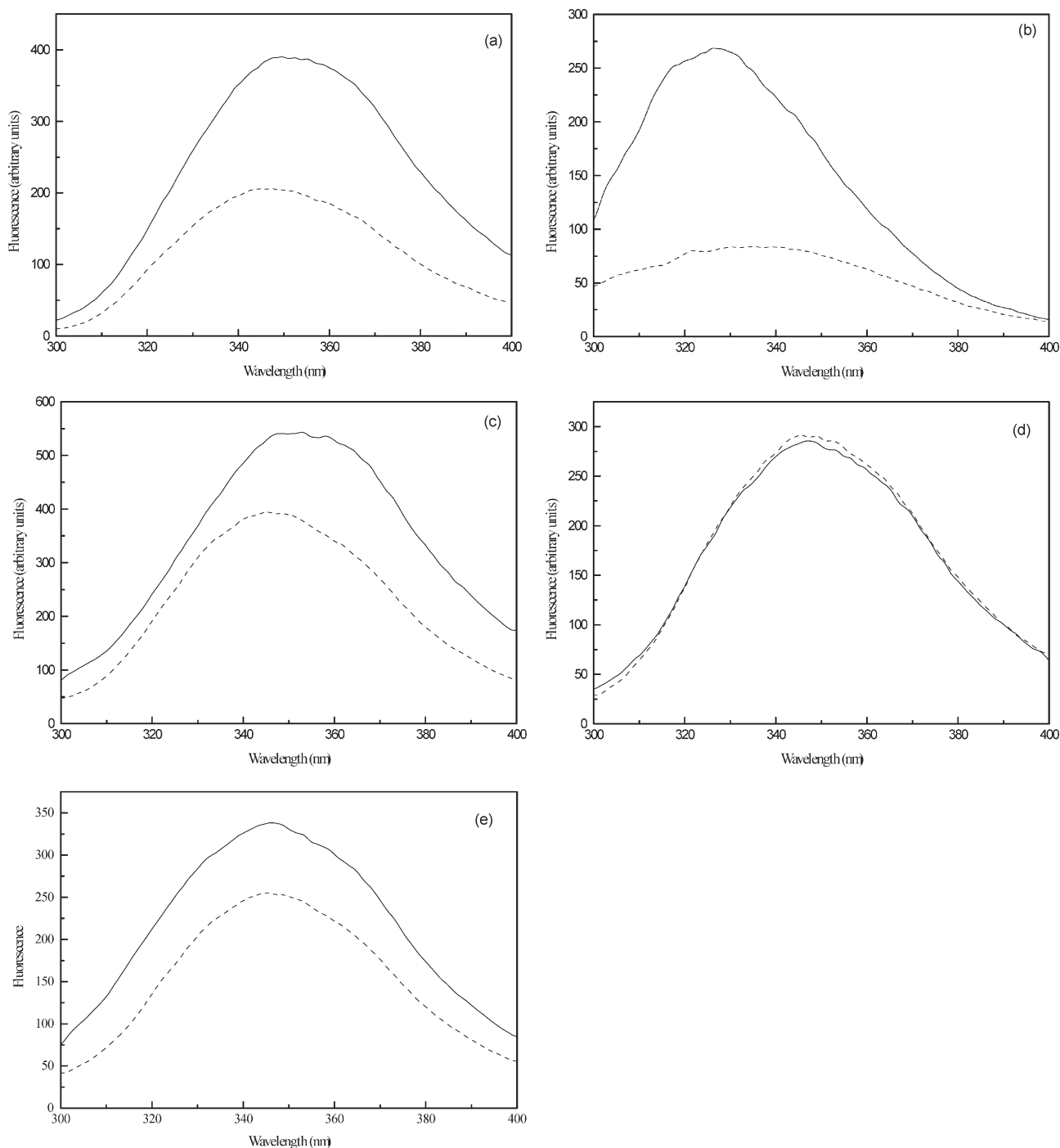


**Fig. 3** Fluorescence properties of the mono-Trp derivatives of ModE in the absence and presence of molybdate. Spectra were recorded at protein concentrations of  $17.6 \mu\text{M}$  ( $0.5 \text{ mg ml}^{-1}$ ) in  $50 \text{ mM Tris/HCl}$ , pH 7.6 at  $20^\circ\text{C}$ , using an excitation wavelength of  $290 \text{ nm}$ . The panels depict the spectra of: (a) unmodified ModE; (b) W186-ModE derivative; (c) W131-ModE derivative; (d) W49-ModE derivative; (e) summed spectrum of the three mono-Trp derivatives. The solid and dashed curves represent the spectra recorded in the absence and presence of  $0.5 \text{ mM}$  molybdate, respectively.

In Fig. 4(e), a comparison is made between the sum of the CD spectra of the three individual single Trp-containing mutant derivatives and the intact wild-type ModE protein. The summed spectra resemble the wild-type enzyme in the absence and presence of molybdate in the characteristic tryptophan region ( $285$  to  $300 \text{ nm}$ ). In addition it can be concluded that on binding molybdate the environments of Trp186 and Trp131 are perturbed. In terms of the effects on shape and amplitude, Trp186 makes the greater contribution to the characteristic molybdate-induced CD spectral change observed for wild-type ModE, consistent with the major effects of molybdate on the fluorescence of this side chain. Addition of molybdate has only a minor effect on the environment of Trp49. These observations are consistent with the location of Trp131 and Trp186 within the molybdate-binding domain and Trp49 in the DNA-binding domain of ModE.<sup>8</sup>

There are marked differences in the summed spectrum and that of wild type ModE between  $260$  and  $285 \text{ nm}$  (Fig. 4(e)). The explanation may simply be that the other aromatic side chains contribute to each of the spectra for the single Trp-containing mutant proteins, but only once to the wild-type protein which contains all three tryptophans.

#### Stoichiometry of molybdate binding to the mono-Trp ModE derivatives

Although the change of Trp49 to Phe in the two mono-Trp derivatives (W186-ModE and W131-ModE) results in the loss of transcriptional activation function, they retain the ability to bind molybdate as evidenced by the changes in the fluorescence emission spectra of these derivatives on addition of molybdate (Fig. 3(b),(c)).

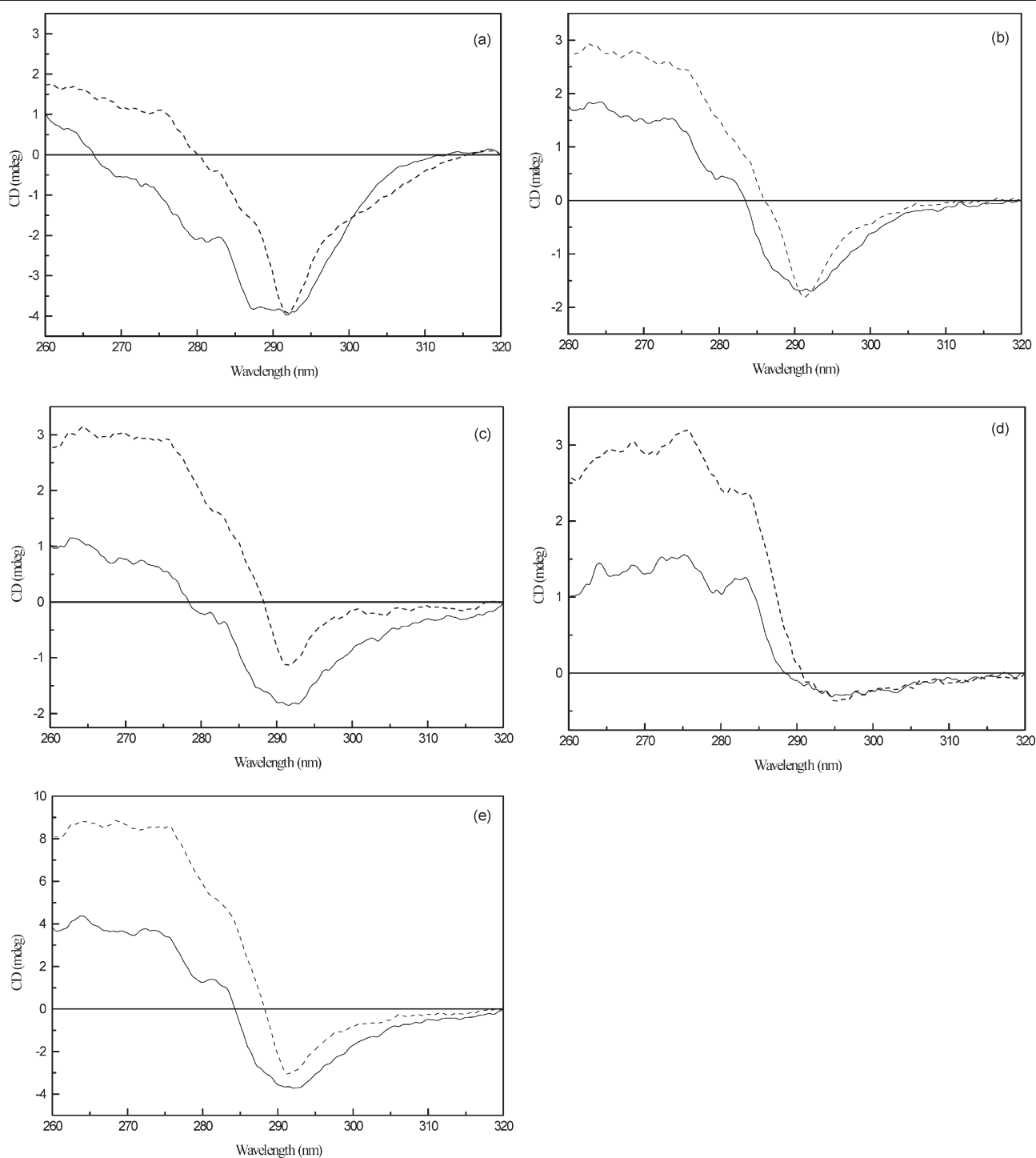


**Fig. 4** Near UV CD spectra of the mono-Trp derivatives of ModE in the absence and presence of molybdate. Spectra were recorded at protein concentrations of  $67.3 \mu\text{M}$  ( $1.9 \text{ mg ml}^{-1}$ ) in a cell of pathlength 0.5 cm in 50mM Tris/HCl, pH 7.6 at 20 °C. The panels depict the spectra of: (a) unmodified ModE; (b) W186-ModE derivative; (c) W131-ModE derivative; (d) W49-ModE derivative; (e) summated spectra of the three mono-Trp derivatives. The solid and dashed curves represent the spectra recorded in the absence and presence of 0.5 mM molybdate, respectively.

Titration of each of these ModE derivatives with molybdate were performed under conditions where  $[\text{ModE}] \gg K_d$  leading to an essentially linear response between fluorescence change and the concentration of added molybdate until saturation is achieved. Analysis of duplicate titrations (Fig. 5) which differed by less than 5% gave rise to binding stoichiometries of  $1.00 \pm 0.05$  and  $1.23 \pm 0.06$  molybdate/ModE monomer and limiting quenchings of 68 and 21% for the W186-ModE and W131-ModE derivatives, respectively. These ModE species retain an ability to bind molybdate similar to that of wild-type ModE.

Under these conditions, the addition of molybdate to the functional W49-ModE gave rise to a small ( $5 \pm 1\%$  in 4 separate experiments) increase in the fluorescence emission intensity. That this increase was indeed due to binding of molybdate was confirmed by

careful titration of the change with increasing molybdate (Fig. 5(c)). The increase saturated at a stoichiometry of  $1.19 \pm 0.06$  molybdate/ModE monomer. This is a significant result because Trp49 is situated at the winged HTH-motif on the DNA-binding N-terminal domain, almost 55 Å remote from the molybdate-binding region of the ModE dimer.

#### DNA-binding affects Trp49 fluorescence

The possibility that Trp49 fluorescence is sensitive to DNA binding was addressed. It was found that addition of a 23-base oligonucleotide containing the recognition site for ModE previously elucidated by footprinting studies (3) (see Materials and methods) to the W49-ModE derivative led to an enhancement of

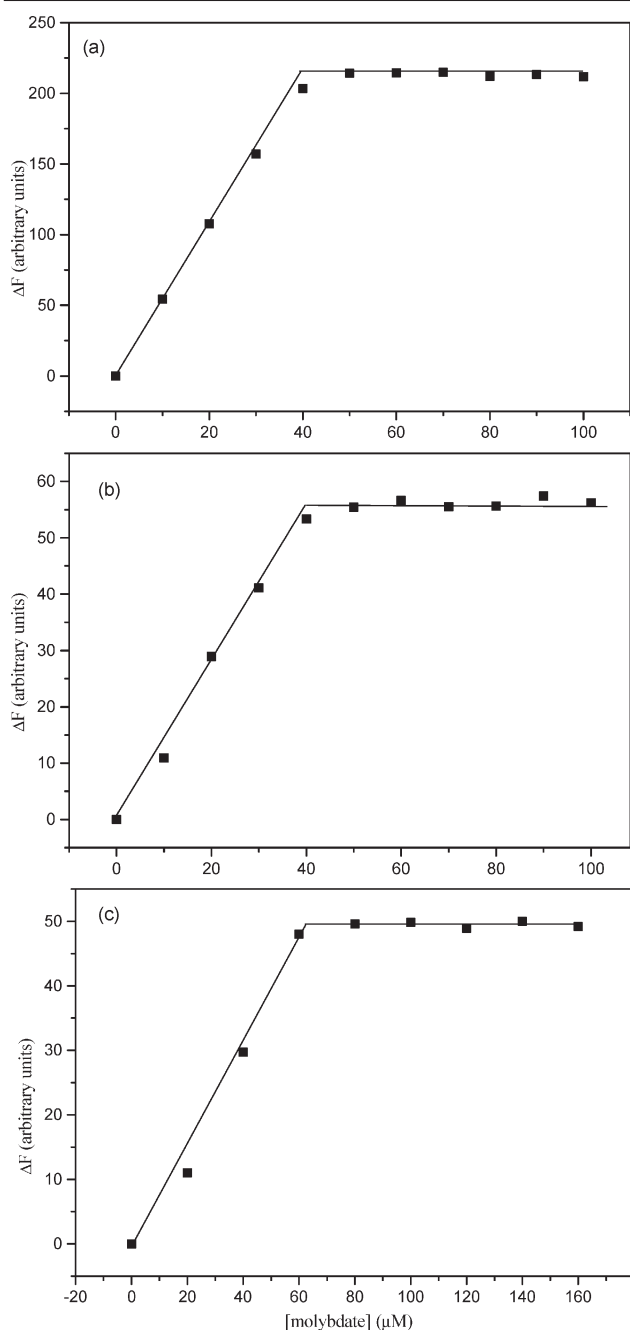


**Fig. 5** Titration of mono-Trp ModE derivatives with molybdate. The concentrations of the ModE derivatives in the cuvette were 39.8, 29.6 and 54.9  $\mu\text{M}$  of ModE monomer for the W186-, W131- and W49-ModE derivatives, respectively. In each case the excitation wavelength was 305 nm and the emission wavelengths were 330, 355 and 348 nm for the W186-, W131- and W49-ModE derivatives, respectively. The limiting fluorescence changes correspond to 68% quenching, 21% quenching and 5% enhancement for the W186-, W131- and W49-ModE derivatives, respectively. Titrations were performed in duplicate with the variation in the degree of saturation at a given concentration of ligand less than 5%; the variation between readings in the duplicate titrations was less than 2% for the W186- and W131-ModE derivatives and less than 5% for the W49-ModE derivative. (a) W186-ModE derivative; (b) W131-ModE derivative; (c) W49-ModE derivative.

the fluorescence of  $8 \pm 1\%$  (3 separate experiments) accompanied by a 2 nm blue shift of the emission maximum (Fig. 6). This reveals that Trp49 experiences small but distinct perturbations arising from both DNA and molybdate binding and is therefore well placed to report on the ligand occupancy at both sites.

#### Effect of DNA on molybdate binding to ModE

Clearly ModE can function internally as a signal transducer effecting changes at the DNA binding site which depend upon the occupancy of the remote molybdate-binding site. The possibility

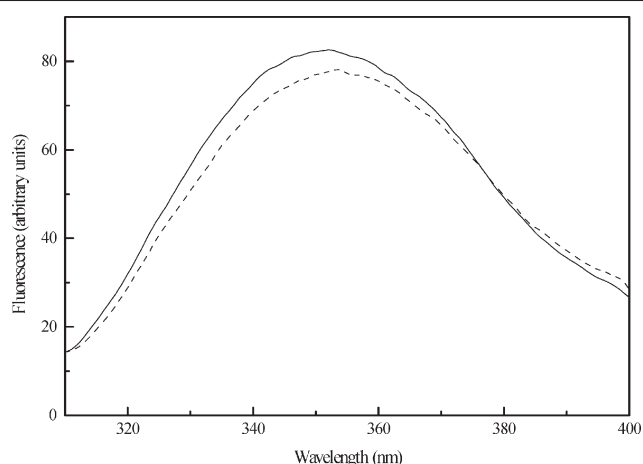


**Fig. 6** The fluorescence of Trp49 senses binding of DNA. The solid and dashed lines correspond to spectra of the W49-ModE derivative (17.6  $\mu\text{M}$ ) recorded in the presence and absence of 4.6  $\mu\text{M}$  DNA. In this and subsequent figures DNA refers to the 23-base oligonucleotide described in the Experimental.

that occupancy of the DNA binding site could likewise influence the binding of molybdate to ModE was assessed by monitoring the changes in fluorescence emission of wild-type ModE on titration with the oxyanion in the presence and absence of an oligonucleotide containing the ModE recognition sequence previously elucidated by footprinting studies (3) (see Materials and methods). The titration curves were analysed in terms of a 1 : 1 model using eqn. (1) as described in Materials and methods. The apparent  $K_d$  of binding of molybdate was reduced from  $1.7 \pm 0.2 \mu\text{M}$  in the absence of DNA to  $0.8 \pm 0.15 \mu\text{M}$  in the presence of 4.6  $\mu\text{M}$  DNA (Fig. 7). The binding of DNA produces a two-fold decrease in the binding constant reflecting a tighter interaction of molybdate with the DNA-ligated ModE than for apo-ModE alone. The concentration of DNA added was as high as could effectively be used without causing excessive inner filter effects and thereby severely reducing the signal-to-noise ratio. Under these conditions (assuming a value of 3.8  $\mu\text{M}$   $K_d$  for the ModE–DNA interaction, see below) the protein would be 50% saturated with DNA. If the experiment could have been reliably performed in the presence of higher (*i.e.* more nearly saturating) levels of DNA, the effect on the  $K_d$  would be more pronounced.

#### Effect of molybdate on the binding of DNA to ModE

The binding of the 23-base oligonucleotide containing the recognition site of ModE, elucidated by footprinting studies,<sup>3</sup> could be monitored by changes in its CD in the region from 240 to 300 nm. Under the conditions employed (4.8  $\mu\text{M}$  DNA and concentrations of ModE up to 15  $\mu\text{M}$ ), the protein makes only a small contribution to the observed CD signal (less than 10%) and this was corrected for by the use of appropriate blanks containing no oligonucleotide. In the absence of ModE, the spectrum of the oligonucleotide is characteristic of B-form DNA, with a maximum at 275 nm and a minimum at 248 nm.<sup>14</sup> On addition of ModE there was an enhancement of the signal, suggesting an increase in the duplex content of the oligonucleotide. The observation of an isobestic point at 258 nm during the titration indicates that only two species are involved (Fig. 8(a)). Similar results were obtained when the titration was performed in the presence of molybdate, except that the increases in ellipticity occur at lower concentrations of added ModE (Fig. 8(b)). Fig. 8(c) shows the increases in ellipticity at 274 nm as a function of added ModE in the absence and presence of molybdate. The titration curves were analysed in terms of a 1 : 1 model for tight ligand binding using Equation 1 as described in Materials and methods (Microcal, Northampton, MA); this analysis yielded values for the dissociation constants of  $3.8 \pm 0.5$  and  $0.7 \pm 0.1 \mu\text{M}$  for the ModE–oligonucleotide complex in the absence and presence of molybdate, respectively. These results indicate that binding of molybdate in one domain of ModE has an effect at the DNA-binding site on the other domain of the protein, and provides direct evidence for inter-site

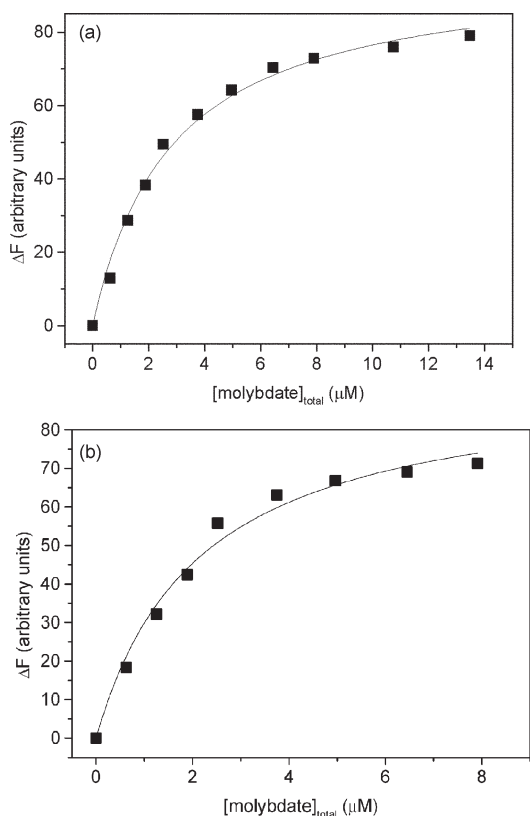


**Fig. 7** Effect of DNA on binding of molybdate to ModE. The binding of molybdate to ModE (1.5  $\mu\text{M}$ ) was monitored by fluorescence with excitation and emission wavelengths of 300 and 353 nm, respectively. Panels (a) and (b) refer to the absence and presence of 4.6  $\mu\text{M}$  DNA, respectively; the data are fitted to a 1 : 1 model for tight ligand binding (Microcal Origin software), with dissociation constants of 1.7 and 0.8  $\mu\text{M}$ , respectively. Spectra were recorded at 20  $^{\circ}\text{C}$  in 50 mM Tris/HCl, pH 7.6.

communication in the protein. It should be noted that the ModE concentrations were not taken to higher values than those shown in Fig. 8 to avoid complications arising from the contributions by the protein to the CD spectra in this spectral region. Our spectroscopic observations are consistent with DNA mobility-shift assays of 127 and 445 bp DNA fragments interacting with ModE in which these longer DNA fragments also present non-specific ModE binding sites.<sup>3</sup>

## Discussion

The generation of the three mono-Trp derivatives of ModE has permitted an assessment of the contributions of each to the substantial quenching (50%) of tryptophan fluorescence observed on binding molybdate. As described earlier, the high resolution crystal structures of the apo-ModE,<sup>8</sup> the oxyanion-ligated (molybdate, tungstate) di-mop C-terminal fragment<sup>9</sup> and the ModE–molybdate complex<sup>10</sup> provide detailed information on the likely structures and immediate environments of Trp131 and Trp186 in the apo- and ligated states. However, high-resolution structural information for Trp49, located at the HTH motif at the DNA-binding N-terminal domain, is presently available only for apo-ModE.<sup>8</sup>

The fluorescence properties of the three tryptophans are distinct both in the presence and absence of molybdate. Trp49 is at the surface of the protein in the HTH motif. The fluorescence properties are consistent with this relatively exposed position. Furthermore the weak near-UV CD spectrum of the W49-ModE derivative suggests that the indole side chain is not significantly immobilized. The addition of molybdate does not significantly influence the UV CD spectrum in the region characteristic of tryptophan, but there is a small (5%) enhancement of its fluorescence with a largely unchanged emission maximum. Clearly Trp49 does not contribute significantly to the overall ligand-induced quenching of the intrinsic fluorescence of ModE. However, Trp49 fluorescence is clearly

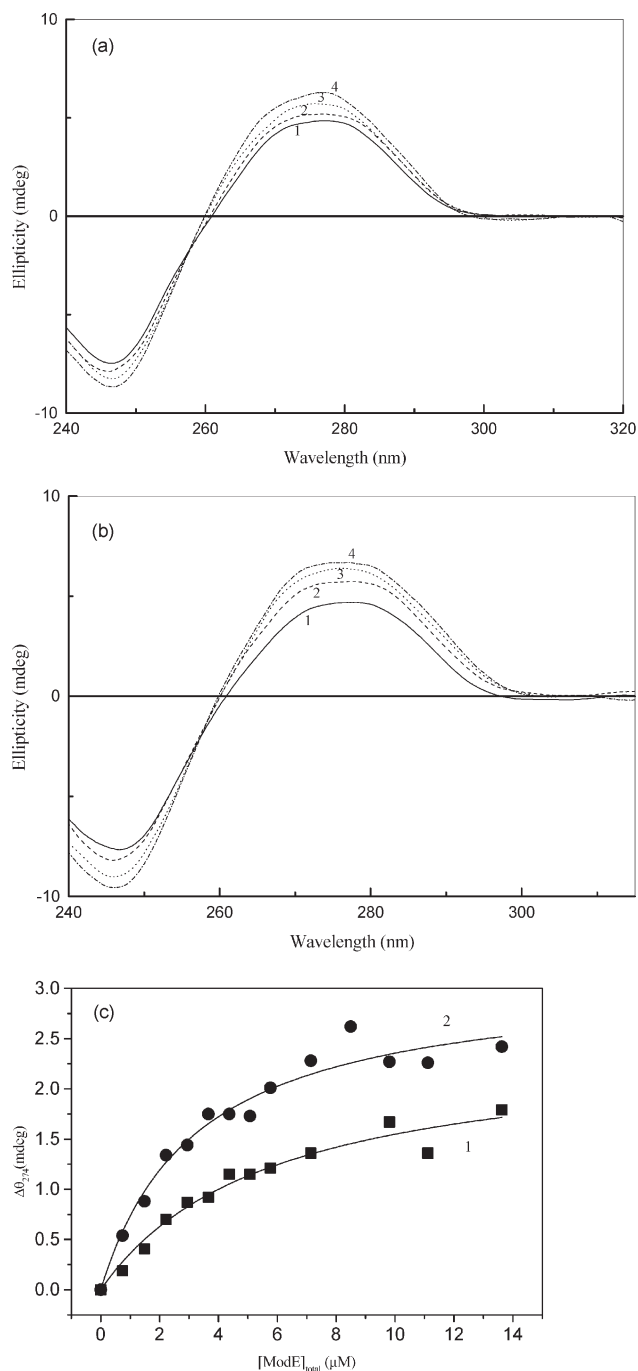


**Fig. 8** Binding of ModE to DNA monitored by changes in the CD spectrum of DNA. The near UV CD spectra of DNA (4.8  $\mu\text{M}$ ) on addition of ModE were monitored in the absence (a) and presence (b) of 50  $\mu\text{M}$  molybdate. In each panel spectra 1–4 represent DNA in the absence of ModE and in the presence of 1.5, 3.6 and 7.1  $\mu\text{M}$  ModE, respectively. In (c), the changes in ellipticity at 274 nm are shown as a function of the total ModE concentration, in the absence (curve 1) and the presence (curve 2) of molybdate. For the sake of convenience, (a) and (b) show only a selection of the spectra used to derive the data plotted in (c). The data in the absence and presence of molybdate are fitted to a 1 : 1 model for tight ligand binding (Microcal Origin software), with dissociation constants of 3.8 and 0.7  $\mu\text{M}$ , respectively. Spectra were recorded at 20  $^{\circ}\text{C}$  in 50 mM Tris/HCl, pH 7.6 in a cell of pathlength 0.5 cm.

sensitive to the occupancy of the molybdate-binding site situated some 55 Å distant in the C-terminal domain of the protein. This communication between the binding sites for DNA and molybdate on ModE is also demonstrated by the synergistic effects in the binding of the two ligands to the protein.

The fluorescence spectrum of Trp131 with an emission maximum at 354 nm suggests a significant exposure to solvent in the apo-protein yet the crystal structure reveals that the indole group of Trp131 is largely buried. A more detailed examination of the

structure reveals that the  $\alpha$ -carbon of Trp131 is reasonably well exposed at the surface of the protein and that there is a significant amount of bound water in the locality; these factors might explain the fluorescence maximum. In contrast to Trp49, the near UV CD spectrum indicates that the mobility of the Trp131 side chain is constrained, consistent with the crystal structure. The motion of this side chain appears further restricted on binding molybdate as revealed by a sharpening of the near UV CD spectrum. The 30% quenching of Trp131 fluorescence on molybdate addition indicates that this region of the protein clearly senses molybdate binding. The blue shift in fluorescence emission maximum to 345 nm on binding molybdate could reflect the exclusion of some of the bound water from the environment of Trp131. From our results it is clear that Trp131 makes a significant contribution to the overall molybdate-dependent quenching of protein fluorescence.

The X-ray structure of apo-ModE indicates that Trp186 is fairly exposed to solvent in a region which is not particularly rich in hydrophobic side chains.<sup>8</sup> The emission maximum for the apo-protein (325 nm) however indicates a markedly non-polar environment. On binding molybdate there are major changes in the fluorescence of Trp186 with a red shift to a broad maximum at 340 nm and a very large (about 70%) degree of quenching. The structural basis for the unusual emission spectrum of the apo-protein is not obvious. One point which may be relevant is the reasonably close proximity within the dimeric ModE of the two Trp186 side chains (within 4 Å) and that the indole rings are in a roughly parallel orientation, permitting some degree of overlap of the delocalised  $\pi$  orbitals. On addition of molybdate the orientation of these two tryptophan residues changes markedly. The crystal structure also suggests that the tryptophan side chains are less mobile in the molybdate-bound state which is consistent with the sharpening of the near UV CD spectrum in the presence of molybdate.<sup>10</sup> According to the side chain analysis undertaken by Singh and Thornton,<sup>15</sup> the occurrence of two Trp side chains with the aromatic rings positioned in a nearly parallel fashion, *i.e.* with an interplanar angle of 0–10° occurs infrequently (approximately 6% of examples in their database). We are not aware of any examples where neighbouring tryptophan side chains in a parallel or nearly parallel orientation occur in the solvent-exposed part of a protein.

Structural analyses of a number of systems involved in the repression or activation of transcription have been carried out.<sup>16,17</sup> In some cases, for example, catabolite activator protein (CAP) there are no large scale conformational changes required for activation and that a straightforward recruitment of RNA polymerase occurs.<sup>18</sup> In other cases, the binding of an effector molecule induces a conformational change that influences complex formation with the target DNA. For some time it has been known that such a conformational change can be induced locally within a DNA-binding domain as exemplified by the *trp* repressor.<sup>19</sup> However, it is now recognised that a ligand-binding event in a domain distant from the DNA-recognition site can result in a structural change in the DNA-recognition moiety of the protein.<sup>20</sup>

The ModE system and the various mono-Trp derivatives of ModE provide a number of possibilities for studying the molecular details of long range communication between domains in a transcriptional activator and thus serves as a useful model system for intramolecular signalling. It would be of future interest to explore the role of key amino acids, especially those in the linker domain (Fig. 1), in relaying the events between the binding domains. Although the observed changes in the affinity of ModE for either molybdate or DNA brought about in the presence of the other ligand are small, it should be noted that they represent underestimates since effective saturation could not be achieved under the constraints of the experimental conditions. In view of what are likely to represent relatively modest changes in the affinity for DNA brought about by the presence of saturating levels of molybdate, it is unlikely that this represents a core feature of ModE's function as an activator. Further work is required to define the mechanism by which the molybdate-ModE complex enhances RNA polymerase activity at the *moa* promoter.

## Experimental

### Bacterial strain and plasmids

The strain LA29 (derived from *E. coli* strain K-12), the pET15b-based plasmid carrying the ModE gene, conditions used for bacterial culture, the enzymes, reagents and recombinant DNA techniques used were as described previously.<sup>3,7</sup>

### Purification of ModE and derivatives

These were purified as fusion proteins with the N-terminal extension MetGlySerSerHis<sub>6</sub>SerSerGlyLeuValProArgGlySerHis. After purification by metal chelate affinity chromatography, the His<sub>6</sub> tag was removed by treatment with thrombin. ModE and its derivatives were separated from the cleaved N-terminal peptide by gel-filtration chromatography on a Superose 12 HR 10–30 column (Pharmacia).

### Protein analysis

Proteins were analysed by SDS-PAGE using a 14% (mass/vol.) separating gel. The concentrations of purified ModE and derivatives were determined spectrophotometrically using the values for the molar absorbance calculated from the appropriate aromatic amino acid composition.<sup>21</sup>

### Circular dichroism spectra

CD spectra of ModE and derivative proteins were recorded at 20 °C on JASCO J-600 600 or JASCO J-810 spectropolarimeters, using cells of 0.5 and 0.02 cm pathlengths and protein concentrations of 67.3  $\mu$ M (1.9 mg ml<sup>-1</sup>) and 17.6  $\mu$ M (0.5 mg ml<sup>-1</sup>) for the near and far UV, respectively. Molar ellipticity values were obtained using the value for the mean residue mass calculated from the amino acid sequence of the appropriate protein. CD spectra of DNA were recorded over the wavelength range 240 to 320 nm in a cell of path-length 0.5 cm.

### Fluorescence measurements

Intrinsic fluorescence spectra were recorded using a Perkin Elmer LS50B spectrofluorimeter maintained at 20 °C. Samples were dissolved in 50 mM Tris/HCl, pH 7.6. The excitation and emission wavelengths are listed in the appropriate figure legends. The binding of molybdate was studied by addition of small aliquots of sodium molybdate to ModE or its derivatives, with the observed values corrected for the effects of dilution (never exceeding 3%). It was not necessary to correct for an inner-filter effect as molybdate does not absorb significantly at the wavelengths used. Titrations were performed in duplicate with the variation in the degree of saturation at a given concentration of ligand less than 5%.

### Analysis of titration data

The equation used to analyse the titration of a ligand L with a fixed concentration of a macromolecule M assuming tight binding with 1 : 1 stoichiometry is:

$$S_{\text{obs}} = (S_{\text{max}}/2M_t) (L + M_t + K_d) - (((L + M_t + K_d)^2 - (4LM_t))^{0.5}) \quad (1)$$

In eqn. (1),  $S_{\text{obs}}$  is the observed change in the spectroscopic signal at a ligand concentration  $L$ ,  $M_t$  is the total concentration of the macromolecule,  $S_{\text{max}}$  is the maximum change in the spectroscopic signal corresponding to complete formation of the ML complex, and  $K_d$  is the dissociation constant. Values of  $K_d$  were obtained by non-linear regression analysis of the titration data using the Microcal Origin (Microcal, Northampton, MA) software.

### Oligonucleotide

A 23 base oligonucleotide (5'-TCGTTATAGATCGATCTATA-ACG-3') containing the recognition sequence for ModE as determined from previous footprinting studies<sup>3</sup> was supplied by Oswel DNA Services, Southampton, UK. It should be noted that this short



oligonucleotide was used in this work in order to minimise potential complications associated with the occurrence of non-specific binding sites for ModE observed in gel shift assays with longer (127 and 445 bp) DNA fragments.<sup>3</sup>

#### Complementation test for plasmid-borne ModE function

Strain LA29 carries a gentamicin resistance-conferring mutation in ModE and an in-frame lacZ reporter gene fusion in the *moa* operon.<sup>7</sup> This strain displays a Lac<sup>-</sup> phenotype (red colony) when grown on lactose-tetrazolium indicator plates.<sup>22</sup> Introduction of a pET15b vector carrying a wild type ModE gene bestows a Lac<sup>+</sup> (white colony) phenotype. Failure to form white colonies on such plates following growth of strain LA29 transformed with a pET15b-based plasmid carrying a mutated ModE gene revealed the loss of ability of the mutated ModE gene product to enhance the expression of *moa*.

#### Site-directed mutagenesis of ModE

The plasmid-borne ModE, pLAA6 was subjected to site-directed mutagenesis using a series of mismatch oligonucleotides with the Stratagene QuikChange<sup>®</sup> site-directed mutagenesis kit. This led to a series of monosubstituted Trp→Phe derivatives at each of the three Trp positions in ModE, namely 49, 131 and 186. These mutations were confirmed by complete DNA sequencing of the ModE gene. The (Trp→Phe) substitution at position 49 resulted in a loss of ModE activity as assessed by the complementation lactose-tetrazolium plate test. Substitutions at positions 131 and 186 were without effect.

In order to construct the series of specific mono-Trp ModE derivatives, the process was repeated on the mono-substituted (Trp→Phe) derivatives to produce the di-substituted derivatives. Again, the mutations were confirmed by complete DNA sequencing of the ModE gene.

#### Abbreviations

CD, circular dichroism; (w)HTH, (winged)helix–turn–helix.

#### Acknowledgements

We thank Alex Schüttelkopf for discussions and Charlie Bond for access to ALINE. This work was supported by grants from the Biotechnology and Biological Sciences Research Council (UK) and from the Wellcome Trust.

#### References

- 1 S. Rech, U. Deppenmeier and R. P. Gunsalus, *J. Bacteriol.*, 1995, **177**, 1023–1029.
- 2 H. M. Walkenhorst, S. K. Hemschemeier and R. Eichenlaub, *Microbiol. Res.*, 1995, **150**, 347–361.
- 3 L. A. Anderson, T. Palmer, N. C. Price, S. Bornemann, D. H. Boxer and R. N. Pau, *Eur. J. Biochem.*, 1997, **246**, 119–126.
- 4 P. M. McNicholas, M. M. Mazzotta, S. A. Rech and R. P. Gunsalus, *J. Bacteriol.*, 1998, **180**, 4638–4643.
- 5 A. M. Grunden, W. T. Self, M. Villain, J. E. Blalock and K. T. Shanmugam, *J. Biol. Chem.*, 1999, **274**, 24308–24315.
- 6 W. T. Self, A. M. Grunden, A. Hasona and K. T. Shanmugam, *Microbiology*, 1999, **145**, 41–55.
- 7 L. A. Anderson, E. McNairn, T. Leubke, R. N. Pau and D. H. Boxer, *J. Bacteriol.*, 2000, **182**, 7035–7043.
- 8 D. R. Hall, D. G. Gourley, G. A. Leonard, E. M. H. Duke, L. A. Anderson, D. H. Boxer and W. N. Hunter, *EMBO J.*, 1999, **18**, 1435–1446.
- 9 D. G. Gourley, A. W. Schüttelkopf, L. A. Anderson, N. C. Price, D. H. Boxer and W. N. Hunter, *J. Biol. Chem.*, 2001, **276**, 20641–20647.
- 10 A. W. Schüttelkopf, D. H. Boxer and W. N. Hunter, *J. Mol. Biol.*, 2003, **326**, 761–767.
- 11 M. R. Eftink and C. A. Ghiron, *Biochemistry*, 1976, **15**, 672–680.
- 12 E. H. Strickland, *CRC Crit. Rev. Biochem.*, 1974, **2**, 113–175.
- 13 R. W. Woody and A. K. Dunker, in *Circular Dichroism and the Conformational Analysis of Biomolecules*, ed. G. D. Fasman, Plenum Press, New York, 1996, pp. 109–157.
- 14 W. C. Johnson, *Circular dichroism and its empirical application to biopolymers*, in *Methods of Biochemical Analysis*, ed. D. Glick, Wiley, New York, 1985, vol. 31, pp. 62–125.
- 15 J. Singh and J. M. Thornton, *Atlas of Protein Side-Chain Interactions*, IRL Press, Oxford, 1992, vol. I and II.
- 16 S. K. Burley and K. Kamada, *Curr. Opin. Struct. Biol.*, 2002, **12**, 225–230.
- 17 J. L. Huffman and R. G. Brennan, *Curr. Opin. Struct. Biol.*, 2002, **12**, 98–106.
- 18 B. Benoff, H. Yang, C. L. Lawson, G. Parkinson, J. Liu, E. Blatter, Y. W. Ebricht, H. M. Berman and R. H. Ebricht, *Science*, 2002, **297**, 1562–1566.
- 19 C. Lawson and P. B. Sigler, *Nature*, 1988, **333**, 869–871.
- 20 P. Orth, D. Schnappinger, W. Hillen, W. Saenger and W. Hinrichs, *Nat. Struct. Biol.*, 2000, **7**, 215–219.
- 21 S. C. Gill and P. H. von Hippel, *Anal. Biochem.*, 1989, **182**, 319–326.
- 22 J. H. Miller, *Experiments in molecular genetics*, Cold Spring Harbor Laboratory Press, Cold Spring Harbor, New York, 1972.
- 23 C. S. Bond, personal communication.
- 24 P. J. Kraulis, *J. Appl. Crystallogr.*, 1991, **24**, 946–950.